LA-UR -79-1306

MASTER

TITLE: DISTRIBUTION OF NUCLEAR CHARGE AND ANGULAR MOMENTUM IN CHAINS 132-137, 99, and 102 OF THERMAL NEUTRON FISSION OF U-235 AT VARIOUS KINETIC ENERGIES AND CHARGE STATES OF THE FRAGMENTS

AUTHOR(S):

See attached list

SUBMITTED TO:

Proceedings of IAEA Conference on Chemistry and Physics of Fission, Jülich, Germany, May 1979.

los alamos
scientific laboratory
of the University of California
LOS ALAMOS, NEW MEXICO 87545

Form No. 836 R2
St. No. 2629
1/78

DEPARTMENT OF ENERGY
CONTRACT W-7405-ENG. 36

Distribution of Nuclear Charge and Angular Momentum in Chains 132-137, 99, and 102 of $^{235}U(n_{th},f)$ at Various Kinetic Energies and Charge States of the Fragments.

H.O.Denschlag, H.Braun, W.Faubel, G.Fischbach, H.Meixler, G.Paffrath, W.Pörsch, N.Weis (Institut für Kernchemie, Universität Mainz, D-6500 Mainz, Germany),
H.Schrader, G.Siegert (Institut Laue-Langevin,Grenoble),
J.Blachot (Centre d'Etudes Nucléaires,Grenoble, France),
Z.B.Alfassi+ (Ben Gurion University,Beer Sheva, Israel),
H.N.Erten+ (Middle East Technical Univ.,Ankara, Turkey),
T.Izak-Biran+ (Soreq Nucl.Research Centre,Yavne,Israel),
T.Tamai+ (Kyoto Univ. Research Reactor Institute,Japan),
A.C.Wahl+ (Washington University,St.Louis,Missouri,USA),
K.Wolfsberg+ (Los Alamos Sci. Lab.,Los Alamos,N.M.,USA).

A b s t r a c t:

The fission product yields of the members of the decay chains 132-137, 99, and 102 in $^{235}U(n_{th},f)$ were measured at various kinetic energies and ionic charge states of the fragments using the mass separator for unslowed fission products 'LOHENGRIN'.

The results are discussed with respect to four aspects:

1. A preferential formation of neutron rich chain members found at high kinetic energy of the fragments is predominantly due to decreasing prompt neutron evaporation. A particularly large effect in chain 132 is attributed to the double shell closure in Sn-132.
2. The persistence of an even-odd pairing effect in the yields throughout the range of kinetic energies studied leads to the conclusion that the high internal excitation energy of the fragments is tied up mainly in the form of collective energy (e.g. deformation energy)rather than single particle excitation.
3. Generally, the yield distribution at constant kinetic energy is invariant with respect to the ionic charge state of the isotopes separated. Deviations from this behaviour found in chains 99,102,133,and 136 are interpreted as being due to Auger events following a converted transition in the decay of ns-isomers taking place in the vacuum of the separator.
4. A pronounced variation of the independent formation ratio of single isomeric states with the kinetic energy of the fragments is providing direct information on the controversial topic of the change of angular momentum of fission fragments as a function of deformation(scission distance).

+ Guest scientist at Universität Mainz.

1. Introduction

Radiochemical yield measurements have been a useful tool in the study of nuclear fission, providing some information on nuclear temperatures and angular momentum at the scission point through the determination of odd-even factors and of isomeric yield ratios.

Radiochemical measurements generally supply information on quantities averaged e.g. over the kinetic energy. The emission of prompt neutrons (or γ-rays) ~~are factors that can be corrected for by~~ correction for is possible in our terms of their average values thus producing a somewhat blurred picture of the initial conditions.

The mass separator LOHENGRIN [1,2,3] may be used to improve this situation as it allows the separation of fission products according to their initial kinetic energy. The total energy of a fission into two given products is constant. In consequence, the kinetic energy of fission fragments is inversely correlated to their internal excitation energy, and a fission fragment pair of particular kinetic energy will possess a well defined total excitation energy and will therefore emit a particular number of neutrons and/or γ-rays. A particular kinetic energy is also presumably connected to a well defined distance of the charge centers at the scission point, i.e. a particular scission configuration.

Measurements of the yield distribution of the light-wing fission products have been carried out at LOHENGRIN using various kinds of dE/dx-detectors [4-11] for the elemental assignment of the isobars. These measurements ~~were~~ concentrated on the mean kinetic energy of the fission fragments, but some measurements at other kinetic energies were included [7,8,10]. The most recent survey will be given in these proceedings[11].

Unfortunately, this method is limited to the light wing fission products because of resolution problems. Therefore, the study of the heavy-region fission products presented in the following is based on a radiochemical method. This method has the disadvantage of depending on the decay characteristics of each single nuclide measured. In consequence, it is much more laborious than the physical methods. It has the other draw-

back that nuclides near stability cannot be measured with high accuracy. It has, however, the advantage that the yields of individual isomers can be differentiated. The possibility of measuring the independent yields of individual isomers has induced us to include light wing chains 99 and 102 into our programme.

2. Experimental

Due to space limitations only the principle approach will be described here, and further details will be given in separate papers [12].

The fission products were produced inside the mass separator LOHENGRIN of the Institut Laue-Langevin in Grenoble. UO_2-targets with a thickness of 40 or 100 $\mu g/cm^2$ were used. In some of the experiments they were covered with a nickel foil of 0,5 µm thickness. In all cases the energy loss of the fragments was determined experimentally by measuring the fragment beam intensity at various kinetic energies and comparing the maximum of the distribution with the most probable kinetic energy of the same mass as obtained by Schmitt et al. [13]. The values of kinetic energies given in this paper have all been corrected for energy loss in the target and due to prompt neutron emission.

The beam of fission products separated according to mass, ionic charge state, and kinetic energy was stopped in a fast transport tape outside the separator. The collection of activity was restricted to a length of 200 mm of tape (as compared to the total length of 720 mm of the exit slit) in order to maintain an energy resolution of ± 1,5% (ca.1 MeV) and to have a uniform deposition profile along the collection length. The collected fission products were transported to a shielded and absolutely calibrated counting position (Ge(Li)-detector and zig-zag mechanism) either continuously or in a start-stop mode, and the γ-rays associated with their β-decay were counted. The velocity of transportation was chosen according to the half-lives of the nuclides studied. Appropriate corrections for growth and decay during collection, trans-

port, and counting, and for detection efficiency allow the calculation of the number of atoms of the individual chain members produced. The fractional yields were obtained by two methods:

a) It was determined from the absolute activity of a descendant with a fractional cumulative yield nearly equal to unity (e.g. ^{134}I, ^{137}Xe, $^{99m+g}Nb$, and ^{135}Xe). Descendants too long-lived for on-line counting (e.g. 78 h - ^{132}Te, 20·8 h-^{133}I, and 9·35 h-^{135}Xe) were (partly) collected on a strip of aluminium foil (generally 25-50 mm wide) maintained fixed during the whole experiment in front of the moving tape system. The activity on this collector strip was measured after the on-line experiment using a well shielded Ge(Li)-detector.

b) In chain 136 this method could not be used due to the stability of Xe. Therefore, the total number of fragments was counted directly by inserting a surface barrier detector into the beam of fragments inside LOHENGRIN.

Method a) is preferred over method b) as it ~~offers~~ is less sensitivity to impurities in the separated masses.

Generally, the limited count rates required a fair detection efficiency (source-to-detector distance ca. 2 cm). This in turn made necessary a careful correction of summing loss [14,15] both in the calibration of the detectors and the actual measurements.

The evaluation of the data relies on the decay properties (half-lives, absolute γ-line intensities, conversion coefficients, branching ratios, etc.) of the nuclides measured. In many cases these ~~constants~~ values were not known and had to be determined in separate radiochemical experiments. Space does not allow the description of these measurements here. The ~~constants~~ values used are, however, given in tabular form (Table I).

3. Results and Discussion

The fractional independent yields obtained will be presented and discussed in two chapters. The first chapter will deal with the influence of the ionic charge state of the fragments

on the yields observed. In the second chapter the variation of the yields with the kinetic energy of the fragments will be treated.

3.1. Fractional independent yields at various ionic charge states of the fragments

~~Generally (i.e.~~ In chains 132, 134, 135, and 137, the yield distribution at constant kinetic energy was found to be invariant with respect to the ionic charge state of the isotopes separated. An example of this type of behaviour is shown in Fig. 1 for chain 134.

In chains 136, 99, 102, and 133, however, a marked dependence of the yields on the charge state of the ions is observed. The results of the first three chains mentioned are shown in Figs. 2 - 4.

Similar effects were observed by Siegert et al. [18] and by Clerc et al. [7,19] for the light-wing fission products. They were explained as being due to the emission of Auger electrons following converted γ-ray-transitions of nanosecond (ns) isomers taking place while these isomers are flying through the vacuum of the separator before entering the magnetic and electric fields (time period from 10^{-14} s until $2{\cdot}10^{-6}$ s after fission). The increase in the mean ionic charge due to the Auger effect will lead to an increased yield of ~~this isotope~~ a nuclide with such an isomeric state at high ionic charge states as is observed for $^{136}I[5^-]$ and $^{136}I[2^-]$ (Fig.2), ^{99}Zr (Fig.3), $^{102}Nb[1^+]$ (Fig.4), and for $^{133m+g}Te$ (not shown). The fact that fractional yields have been plotted leads to seemingly decreasing yields for the other unaffected isotopes (^{136}Xe, ^{136}Te in Fig.2, ^{99}Y in Fig.3, ^{102}Zr, $^{102}Nb[h]$ in Fig.4). The yields of the isomers of ^{99}Nb (Fig.3) appear to be practically constant. This could be interpreted as indicating the presence of another - less effective - isomeric transition in that chain feeding the two isomers and compensating for the expected decrease in yield. In this context it is interesting to note that in chain 102 the ns-isomer seems to be feeding only the low-spin isomer of Nb whereas in chains 99

and 136 both isomers are apparently fed to nearly the same extent. It should be stated here that the results concerning chain 102 require further confirmation as they are based on preliminary information concerning the decay characteristics (see Table I). In the present examples as in the cases identified in Refs.[18] and [19] ns-isomers that could be responsible for the effect have been detected independently by Clark et al. [20] (Table II).
However, the identification of these isomers is not fully conclusive as numerous additional ns-isomers have been detected [20], in particular in chains 132, 134, 135, and 137. These chains, however, have shown no dependence on the ionic charge state.
It seems desirable to give additional support to the interpretation given above, e.g. by measuring the half-life of the parent assumed responsible for the increased ionic charge. This can be done by introducing into LOHENGRIN a thin foil which will re-equilibrate the ionic charge of the ions in flight. A 're-equilibration' prior to the decay of the isomer will not affect the increased average charge while a re-equilibration after decay will remove the effect. Therefore, the measurement of the average ionic charge as a function of the target-to-foil distance will allow the calculation of the desired lifetime as the velocity of the ions can be calculated from their energy.

3.2. Fractional independent yields at various kinetic energies of the fragments

The yields measured for the various fission product chain members and kinetic energies are given in Table III.
The yields indicated refer to the cumulative yield of the last chain member shown. This yield can generally be assumed to be identical with the chain yield. In some cases, however, (e.g. in chain 133 at low kinetic energy), the independent yield of the subsequent chain member (^{133}I) is not negligible even though it could not be measured. In these cases, possible effects on Z_p-values and odd-even/even-odd factors discussed subse-

quently have been taken into account.
Generally, the yields of individual isomeric states are indicated in Table III. In two cases (chains 134 and 135), however, the yields of the individual isomers had to be determined in separate experiments, and therefore the fragment kinetic energies were not identical. In these cases the yields (^{135}Xe) or the fraction of high spin isomer relative to the total,

$$F_h = \frac{Y_{FI}(\text{high spin isomer})}{Y_{FI}(\text{both isomers})}$$

are given separately in Table III.
In general, good agreement is observed between radiochemical yield values [21] and the yields obtained in the present experiments at the mean kinetic energy of the fragments. There is also general agreement concerning chains 99 and 102 with the data obtained at LOHENGRIN (at mean kinetic energy) using physical methods [6,8].
A typical example of the change in yields with varying kinetic energy of the fragment is shown in Fig.5. This example has been chosen as it allows a comparison with results of Clerc et al. [7,7a] at two kinetic energies of the fragments. The agreement seems reasonable. Other measurements at other kinetic energies [8] agree in their trends. Some deviations at low kinetic energies are presumably due to the use of a thick UO_2-target (400 $\mu g/cm^2$) and the consequent loss in energy resolution.
The trends observed in Fig.5 and common to all chains studied (Table III) is an increase with increasing kinetic energy of the (neutron-rich) chain members with the lowest nuclear charge at the expense of the chain members of higher nuclear charge. The slight maximum found for the intermediate chain member ^{99}Zr resulting from some gain in yield from ^{99}Nb and some subsequent loss to ^{99}Y at higher energies is found even more pronounced in other chains (e.g. chain 132). The observed effects are among other reasons due to the decrease in prompt neutron emission with decreasing excitation energy (increasing kinetic energy) of the fragments.
Besides the change in element yields mentioned, a strong va-

ration in the independent yields of isomeric states is observed ~~here~~ for the first time. This effect consisting of a decrease of ~~the fraction~~ $Y_{h\ell}/Y$ ~~of the high spin isomer relative to the total yield of the isotope~~ and observed in chains 99, 102, 132, 133, 134, 135, and 136 (Table III) is illustrated in Fig.6 for chain 134.
In the following, ~~a discussion~~ the changes in yields will first be ~~given of the changes in yields~~ discussed in terms generally used for a discussion for a discussion of charge distribution in nuclear fission, i.e. Z_p, σ, and ~~odd-even~~ even-odd factors (EOF) [22,23,24]. Finally, the changes in the independent yields of isomers will be discussed with respect to the angular momentum of the fission fragments and scission point configurations.
In order to study the effects of kinetic energy on the charge distribution, the yields observed were fitted to a Gaussian type curve modulated by ~~odd-even~~ even-odd factors as given below.

$$(1) \qquad FI(Z) = N^{-1} \int_{Z-1/2}^{Z+1/2} EOF(Z)\cdot P(Z)\cdot dZ \quad , \quad \text{and}$$

$$(2) \qquad FC(Z) = N^{-1} \int_{Z=-\infty}^{Z+1/2} EOF(Z)\cdot P(Z)\cdot dZ$$

$$\text{with:} \quad P(Z) = (2\pi\sigma^2)^{-1/2}\cdot \exp[-0{,}5\cdot((Z-Z_p)/\sigma)^2].$$

FI (FC): fractional independent (cumulative) yields.
N is a normalisation factor assuring that the sum of all fractional independent yields within one chain remains equal to unity after the modulation by ~~odd-even~~ even-odd factors.

$$N = \int_{Z=-\infty}^{Z=+\infty} EOF(Z)\cdot P(Z)\cdot dZ$$

This curve is described completely by a set of three variables:

Z_p: the most probable charge,
σ : the width parameter of the curve, and
EOF: the even-odd pairing factor.

Calculation of the three parameters requires the knowledge of at least four yields. However, the present experiments provide only two or three element yields per chain (Table III). Therefore, only some of the constants could be calculated explicitly+. Whenever three yields were ~~known~~ measured both Z_p and EOF were calculated. In the other cases only Z_p was calculated. In these cases the ~~assumption~~ odd values of σ and/or EOF was based on independent information, e.g. the radiochemical yield distribution. Fortunately, the results obtained for Z_p are quite insensitive to the assumed values of σ and/or EOF since the yields used were those of the most prominent chain members. Even the simple calculation of the average nuclear charge $\overline{Z}$ according to [5,9] leads to almost identical results. Although the absolute size of EOF is sometimes affected by the choice of σ, fortunately the change in EOF with the kinetic energy of the fragments is practically not affected as long as σ itself does not vary with energy.

The present method of evaluation is preferred over the method used in Refs. [5] and [9], because it allows the handling of incomplete sets of data more easily in a self-consistent way. The main advantage of the present method is, however, that it provides a well-defined EOF-value, whereas the other method uses the oscillation of σ', the square root of the second moment of the charge distribution, to obtain an ~~odd-even~~ even-odd factor in a ~~more~~ less indirect way.

The resulting Z_p ~~values~~ and EOF ~~factors~~ values are given in Table III. The Z_p values are plotted in Fig.7 versus the deviation from average fragment kinetic energy $(E_k - \overline{E}_k)$. The data points in the figure may be compared with a drawn-out line representing Z_{UCD}, the nuclear charge calculated assuming unchanged charge density according to the equation:

$$(3) \quad Z_{UCD}(E_k) = (A + \nu_A(E_k)) \cdot \frac{Z_F}{A_F} \quad , \quad \text{with:}$$

$$\nu_A(E_k) = \bar{\nu}_A - \frac{E_k - \overline{E}_k}{7} \quad , \text{ when } \bar{\nu}_A - \frac{E_k - \overline{E}_k}{7} \text{ positive, else } \nu_A(E_k) = 0.$$

+ The calculation was carried out using the fit-programme ORGLSW.

strong effects (A = 132, 134, 136, and 137). The most interesting result is certainly the observation that the effect is apparently preserved over the whole span of kinetic energies which indicates that the internal excitation energy of more than 15 MeV (corresponding to low kinetic energy) is tied up almost exclusively in collective degrees of freedom, e.g. deformation energy. The results in chains 132 and 137 showing an apparent minimum in the even-odd factors around $\bar{E}_k$ could be interpreted as supporting results of Nifenecker et al. [27] indicating that the 'intrinsic excitation energy' (total energy minus kinetic (coulombic) and deformation energies) shows a maximum for those fragments carrying the mean kinetic energy. However, the results of chain 134 contradict this interpretation and the results of chain 136 do not support it. Measurements of more chains are needed to answer this question.

One of the most interesting results of the present work certainly concerns the independent yields of the individual isomers and their variation with kinetic energy.

Using the formalism developed by Huizenga and Vandenbosch [28,29] and the equations as explicitly written down in [30] the ratios of independent yields of the isomers as given in Table III were converted into the root mean square angular momentum (J_{rms}) of the fission fragments. The resulting values are plotted in Fig.9 as a function $E_k - \bar{E}_k$.

The values obtained for the mean kinetic energy of the fragments ($E_k - \bar{E}_k = 0$ in Fig.9) cluster around 6-7 $\hbar$ for the heavy fission products and somewhat less for the light fission products in agreement with results obtained by other groups, e.g. Wilhelmy et al. [31]. The unusually low value of J_{rms} for ^{99}Nb may be due to nonstatistical effects in the deexitation of ^{99}Nb fission fragments [32,28].

The most striking effect observed in Fig.9 is the pronounced decrease in J_{rms} by about 3 $\hbar$ per 10-15 MeV. This effect, expected on theoretical grounds [31,33,34], has long been debated since the limited experimental information available was contradictory. Wilhelmy et al. [31] concluded from the rela-

A mass number of fission product.

$\nu_A(E_k)$ number of prompt neutrons emitted for chain of mass A at kinetic energy E_k.

$\bar{\nu}_A$ mean number of prompt neutrons emitted for chain A (from [22]).

Z_F, A charge (mass) of compound nucleus.

The relation assumes that about 7 MeV have to be spent in order to evaporate a neutron [25]. It could be shown that the number of neutrons emitted at the mean kinetic energy $\bar{E}_k$ corresponds to the mean number of neutrons emitted at all kinetic energies.

The distance between the experimental points (Z_p) in Fig.7 and the line (Z_{UCD}) represents the parameter ΔZ ($= Z_p - Z_{UCD}$) used to describe the charge polarisation in the fissioning nucleus [22].

At a first glance the change in Z_p (data points) is essentially parallel to the change in Z_{UCD} indicating that the decrease in prompt neutron emission ~~diminishing~~ with decreasing excitation energy of the fragments has the dominating influence on the variation of the experimental yields observed and that the distribution of protons and neutrons at scission is roughly independent of the scission distance. Looking more closely, however, one finds deviations from this simple behaviour.

(1) The Z_p-values in chains 137, 136, and 134 seem to approach the Z_{UCD}-line at high kinetic energies. This trend was actually predicted for all chains by Wilkins et al.[26]. The differences in the behaviour of neighbouring chains can possibly be attributed to an uneven distribution of excitation energy among complementary fragments [27].

(2) In chain 132 the opposite effect is found: the gap between Z_p and Z_{UCD} somewhat widens at high kinetic energies, when prompt neutron emission has ceased. Possibly this is due to the influence of the double shell closure in $^{132}_{50}Sn^{82}$.

The odd-even factors given in Table III are plotted in Fig.8 versus $E_k - \bar{E}_k$.

The behaviour is somewhat complicated as was also found for the light-wing fission products [5,9]. Chains showing practi-

There are

tive intensities of ($6^+ \rightarrow 4^+ \rightarrow 2^+ \rightarrow 0^+$) ~~ground state~~ transitions cascade at three kinetic energy intervals (total spin 20-30 MeV for heavy or light fragment) that the value of J_{rms} is on the average (within $\pm$ 1 $\hbar$) independent of the fragment total kinetic energy. Nifenecker et al.[27], however, estimated from the correlation of the total γ-ray energy and the neutron multiplicity in the fission of ^{252}Cf and ^{235}U that the average spin of the fission fragments should increase by one unit for an increase of excitation energy of approximately 7 MeV (corresponding to a $\Delta J_{rms}/\Delta E \approx 0{,}14$ $\hbar$/MeV). The results of the present work based on a fit of data points in Fig. 9 are compiled in Table IV. There is general agreement with the value of Nifenecker. A comparison of the values obtained for individual chains could possibly be used to provide information on fragment stiffness at the scission point.

Tabelle mit Punkt

Figure captions:

Fig. 1: Fractional cumulative (Sb) and ~~independent~~ (Te,I) yields in chain 134 at various ionic charge states of the fragments. Kinetic energy $E_k = 77 \pm 2$ MeV.

Fig. 2: Fractional cumulative (Te) and ~~independent~~ (I,Xe) yields in chain 136 at various ionic charge states of the fragments. Spin and parity of iodine isomers indicated in brackets. $E_k = 75 \pm 2$ MeV.

Fig. 3: Fractional cumulative (Y) and ~~independent~~ (Zr,Nb) yields in chain 99 at various ionic charge states of the fragments. Spin and parity of Nb-isomers indicated in brackets. $E_k = 102 \pm 7$ MeV.

Fig. 4: Fractional cumulative (Zr) and ~~independent~~ (Nb) yields in chain 102 at various ionic charge states of the fragments. Assumed spins and parities of Nb-isomers indicated in brackets. $E_k = 102 \pm 5$ MeV.

Fig. 5: Fractional cumulative (Y) and ~~independent~~ (Zr,Nb) yields in chain 99 at various kinetic energies of the fragments ($q = 21^+$). Blank points from [7,7a], full points this work.

Fig. 6: Fraction of independent yield of $^{134}I[8^-]$ relative to total independent yield of $^{134}I[8^-]$ and $[4^+]$ at various kinetic energies of the fragments.

Fig. 7: Z_p-values (data points) from Table III and Z_{UCD} (drawn-out line) as calculated from Eq.(2) at various kinetic energies of the fragments (E_k). For a better comparability the kinetic energies have been normalised to the mean kinetic energy ($\overline{E}_k$) of the fragments of the same mass (from [13]).

Fig. 8: Odd-even factors (EOF-values) from Table III at various kinetic energies of the fragments (E_k). For a better comparability the kinetic energies have been normalised to the mean kinetic energy ($\overline{E}_k$) of the fragments of the same mass (from [13]).

Fig. 9: Root mean square angular momentum of fission fragments calculated from the independent formation ratios of single isomeric states characterised by their spins and parities at various kinetic energies of the fragments (E_k). For a better comparability the kinetic energies have been normalised to the mean kinetic energy ($\overline{E}_k$) of the fragments of the same mass (from [13]). The results on Nb-102 are based on preliminary decay characteristics and have been calculated for two values of

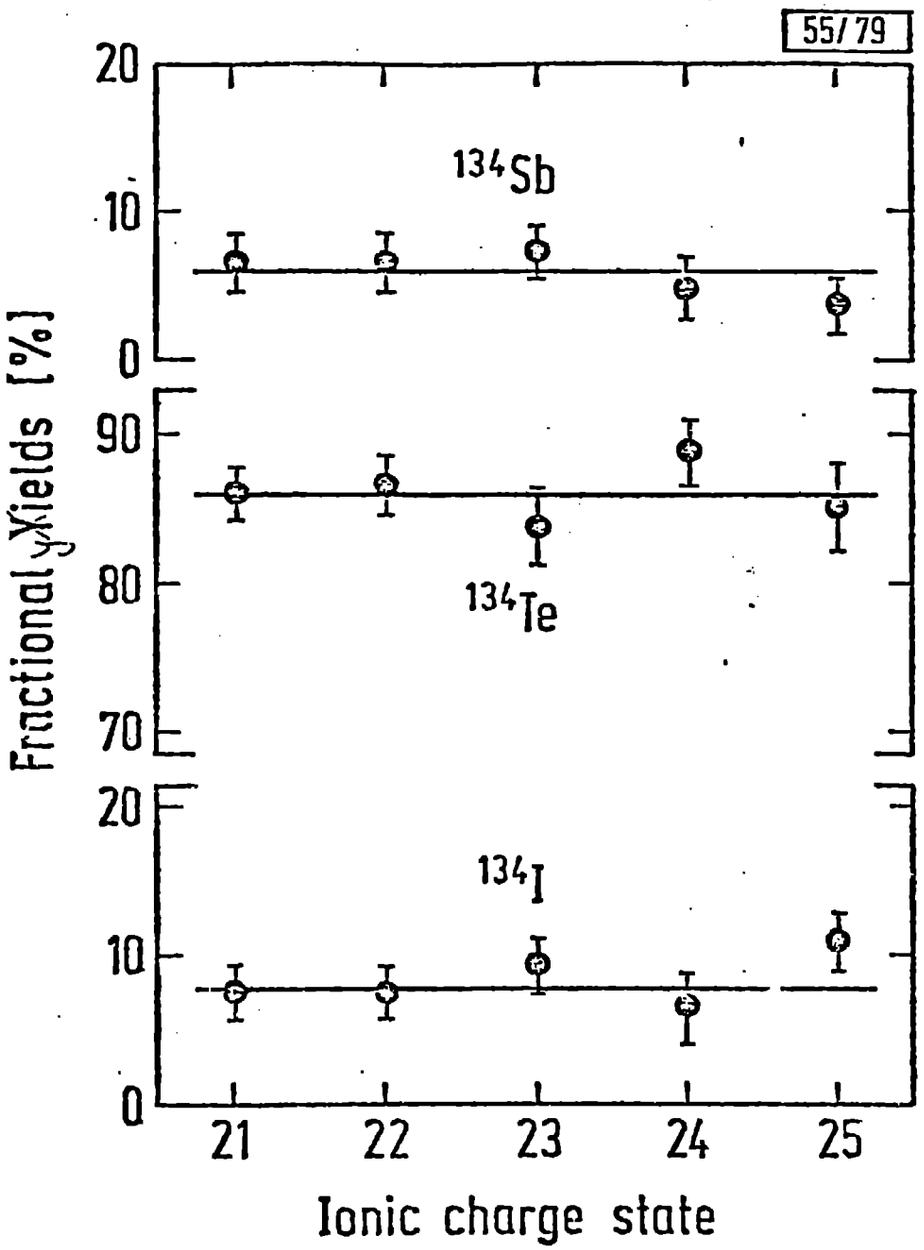
55/79
20
10
0
^{134}Sb
90
80
^{134}Te
70
20
10
0
^{134}I
Fractional γ-Yields [%]
21
22
23
24
25
Ionic charge state

Fig. 1

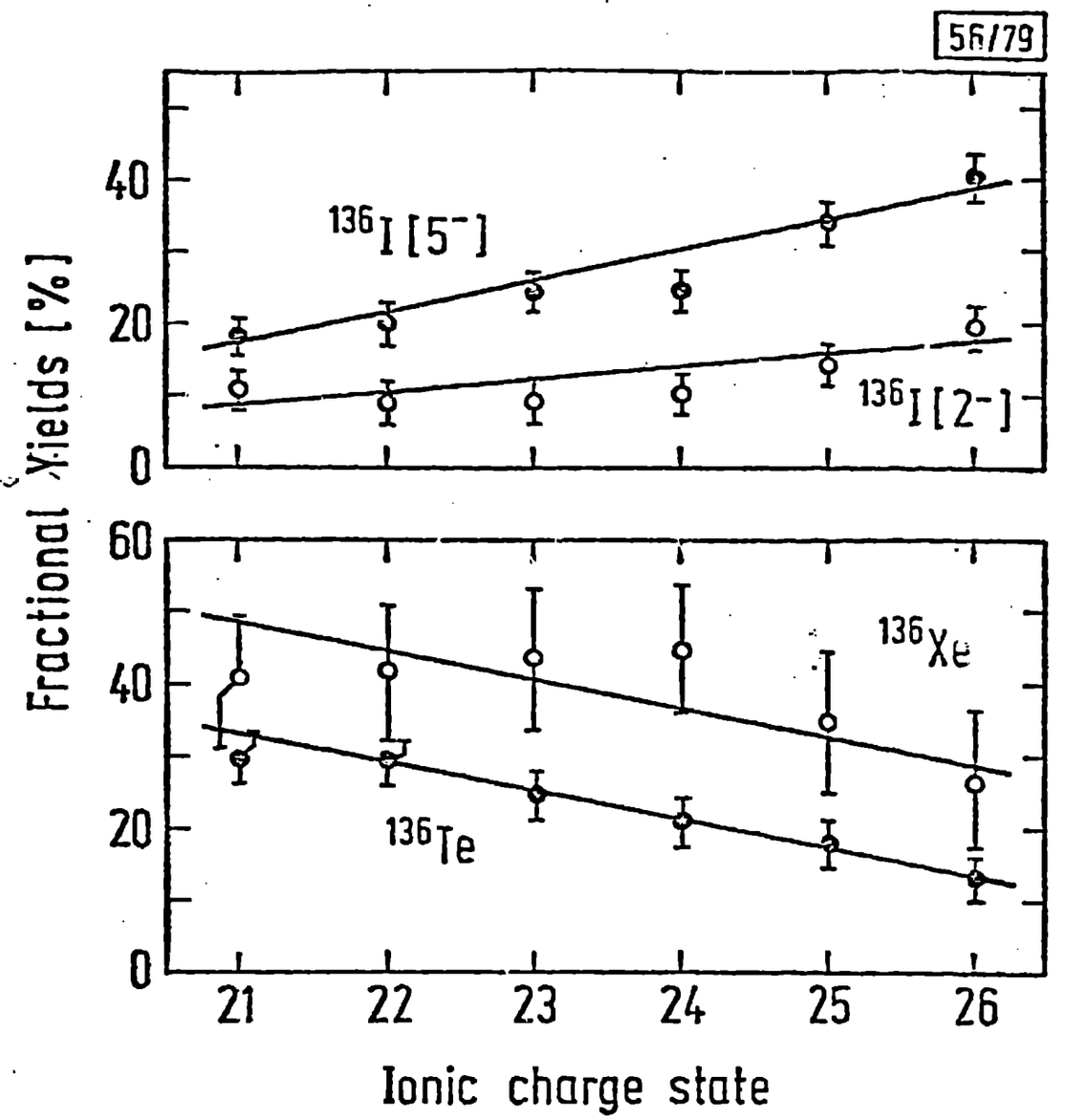
56/79
40
20
0
^{136}I [5$^-$]
^{136}I [2$^-$]
Fractional Yields [%]
60
40
20
0
^{136}Xe
^{136}Te
21
22
23
24
25
26
Ionic charge state

Fig. 2

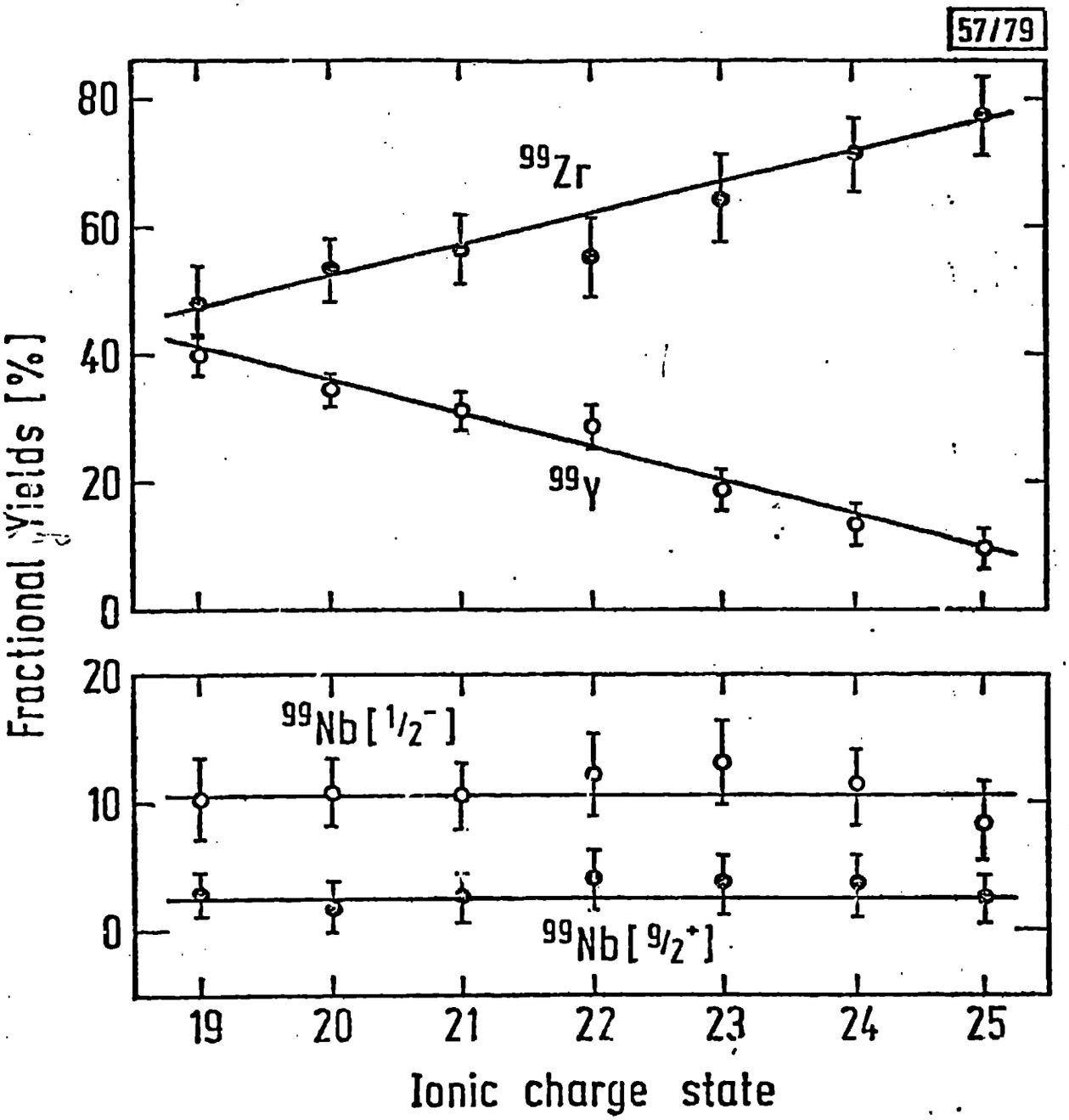
57/79
80
60
40
20
0
Fractional Yields [%]
^{99}Zr
^{99}Y
20
10
0
^{99}Nb [1/2$^-$]
^{99}Nb [9/2$^+$]
19
20
21
22
23
24
25
Ionic charge state

Fig. 3

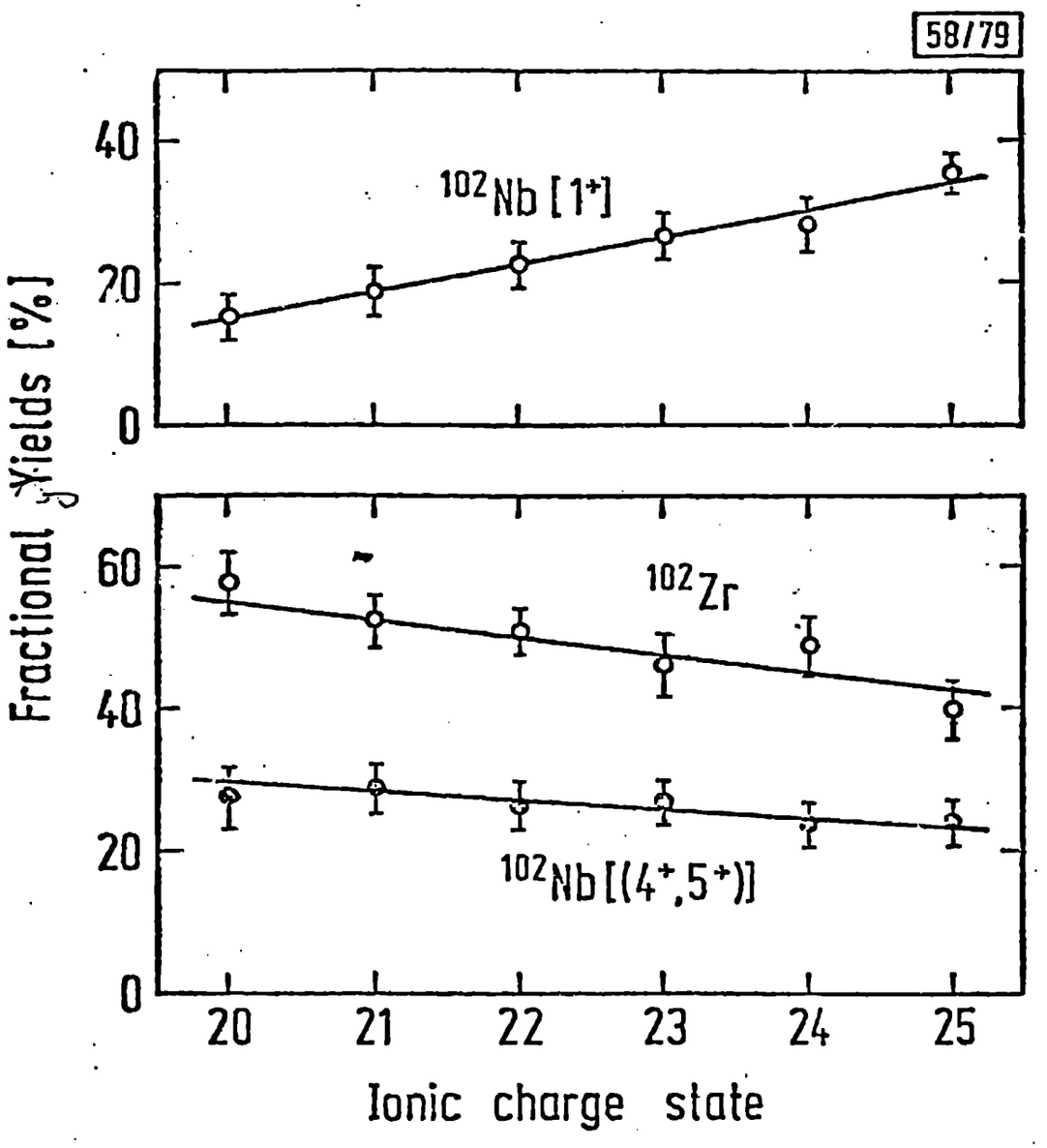
58/79
40
20
0
^{102}Nb [1$^+$]
Fractional Yields [%]
60
40
20
0
^{102}Zr
^{102}Nb [(4$^+$,5$^+$)]
20
21
22
23
24
25
Ionic charge state

Fig 4

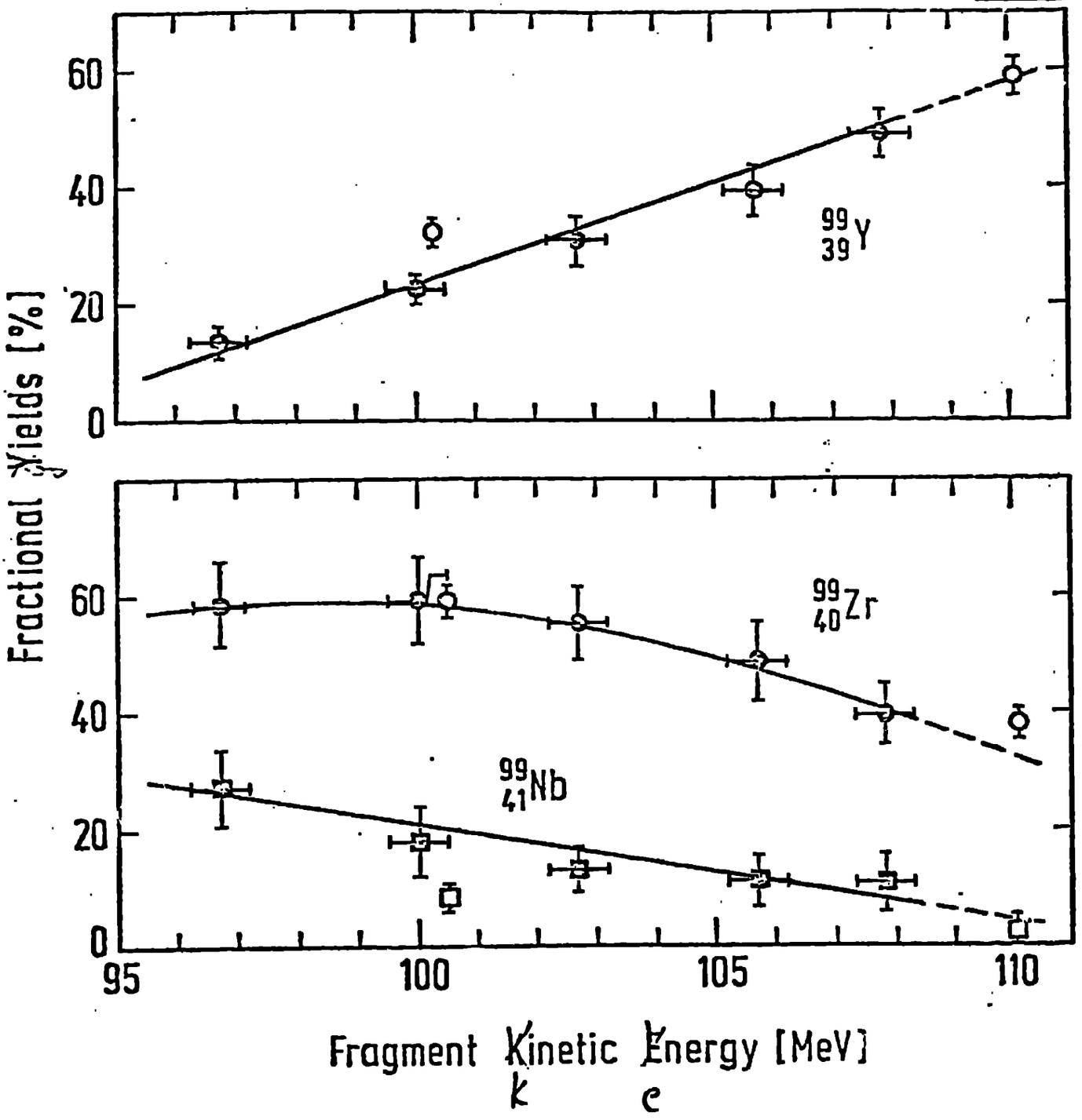
60
40
20
0
$^{99}_{39}Y$
60
40
20
0
$^{99}_{40}Zr$
$^{99}_{41}Nb$
95
100
105
110
Fractional Yields [%]
Fragment Kinetic Energy [MeV]

Fig 5

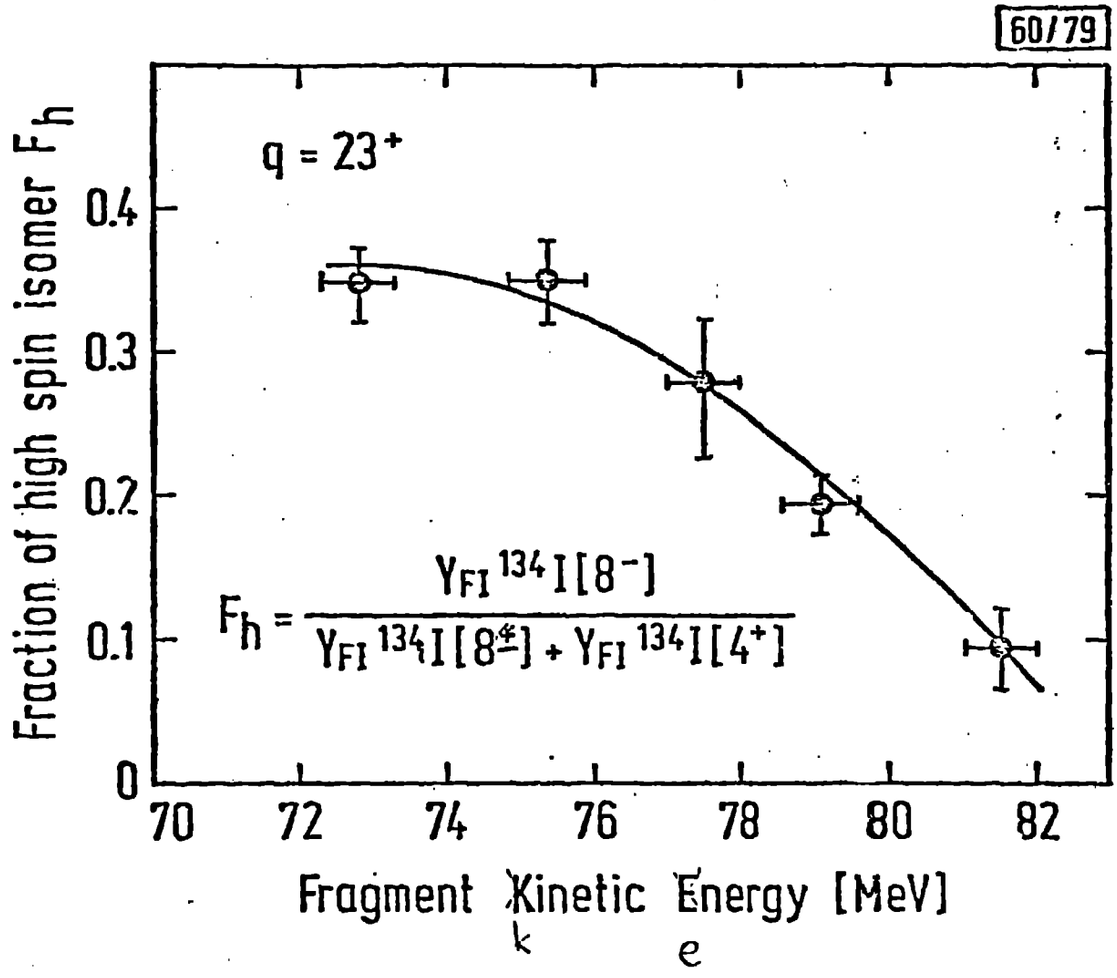
60/79
q = 23+
Fraction of high spin isomer Fh
0.4
0.3
0.2
0.1
0
70
72
74
76
78
80
82
Fragment Kinetic Energy [MeV]
Fh = YFI 134I[8−] / (YFI 134I[8±] + YFI 134I[4+])

Fig.6

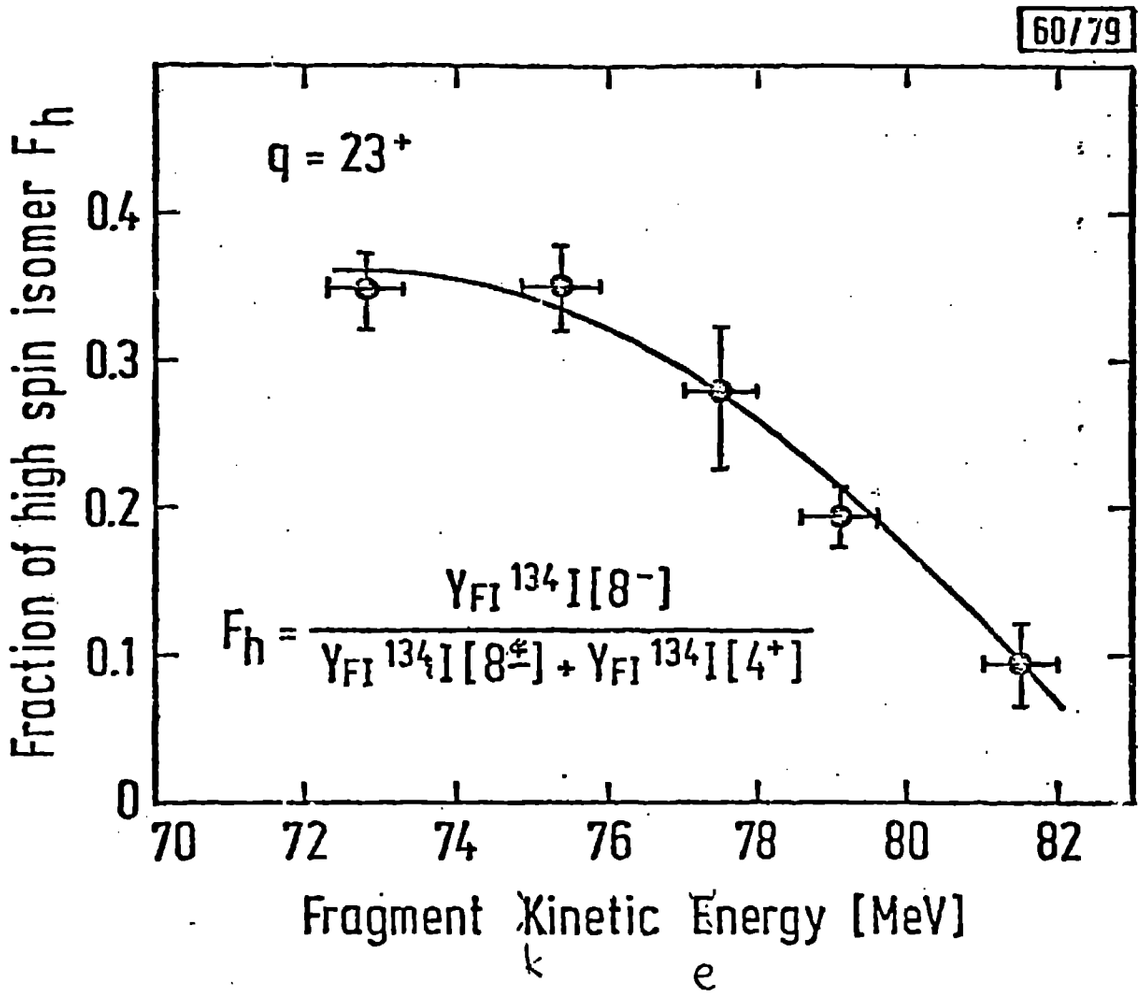
60/79
q = 23+
Fraction of high spin isomer Fh
0.4
0.3
0.2
0.1
0
70
72
74
76
78
80
82
Fragment Kinetic Energy [MeV]
Fh = YFI 134I[8−] / (YFI 134I[8±] + YFI 134I[4+])

Fig.6

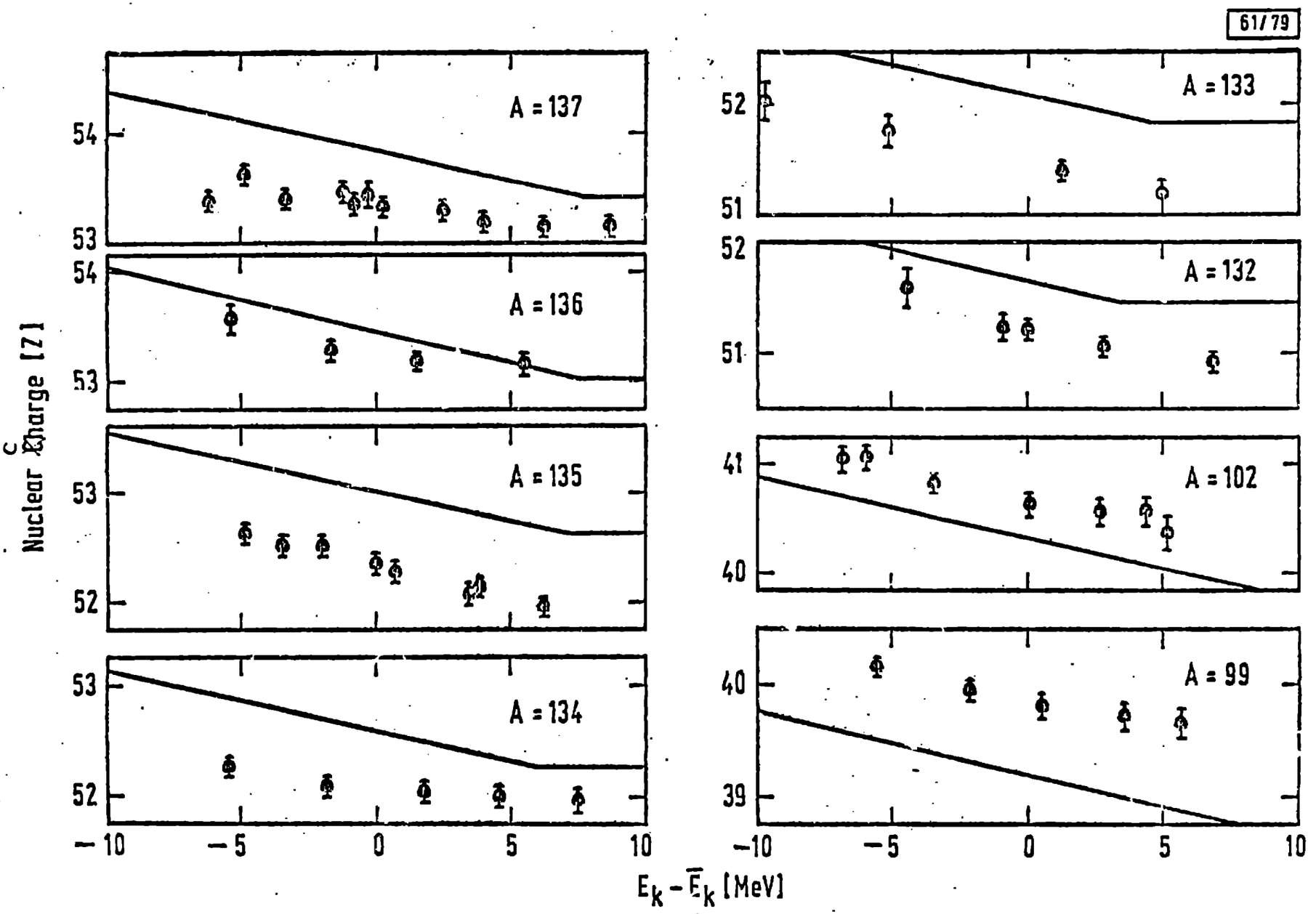
A = 137
A = 136
A = 135
A = 134
A = 133
A = 132
A = 102
A = 99
Nuclear Charge [Z]
$E_k - \bar{E}_k$ [MeV]

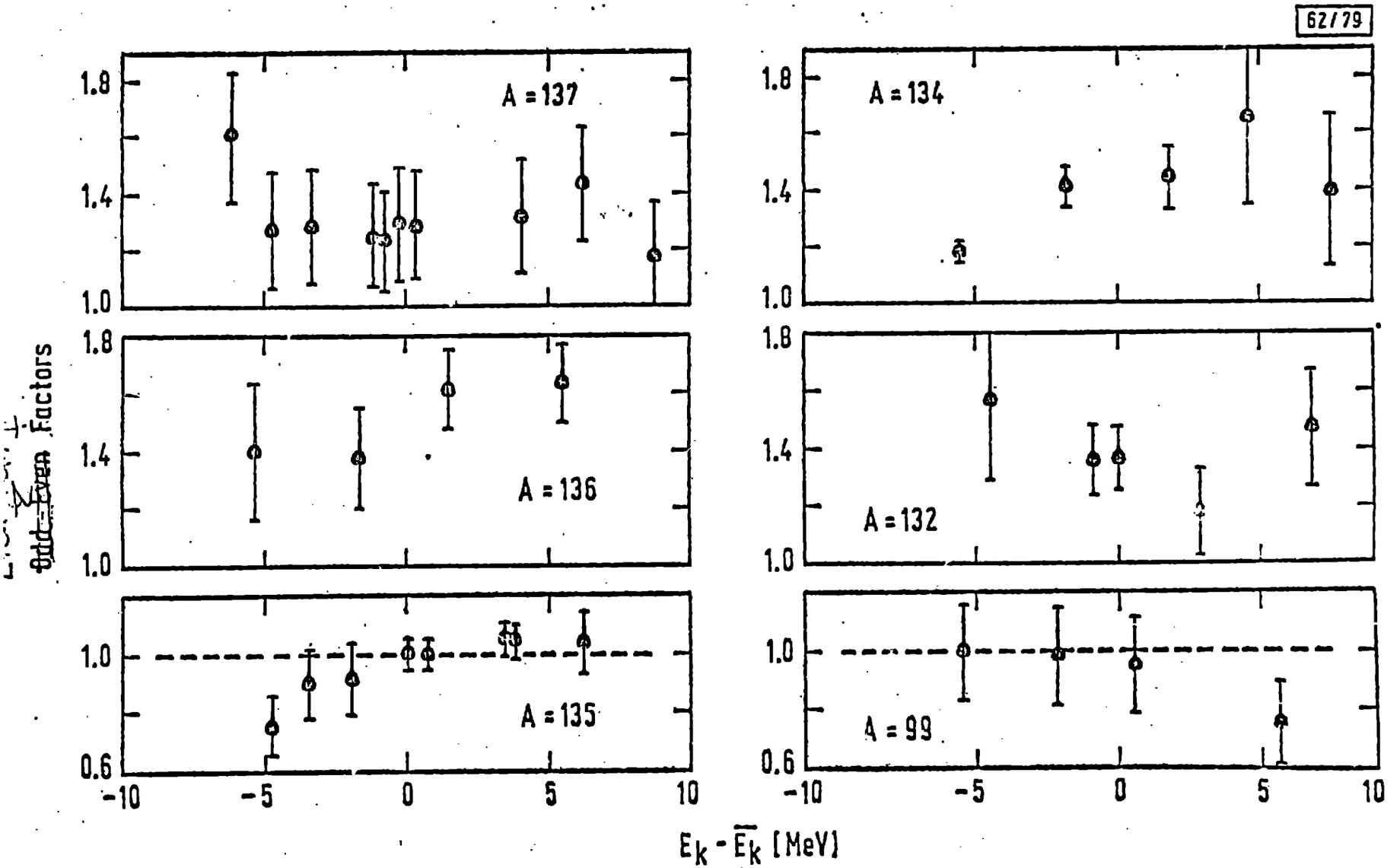

Fig. 8

Strich Bilde mehr über dem „E"!

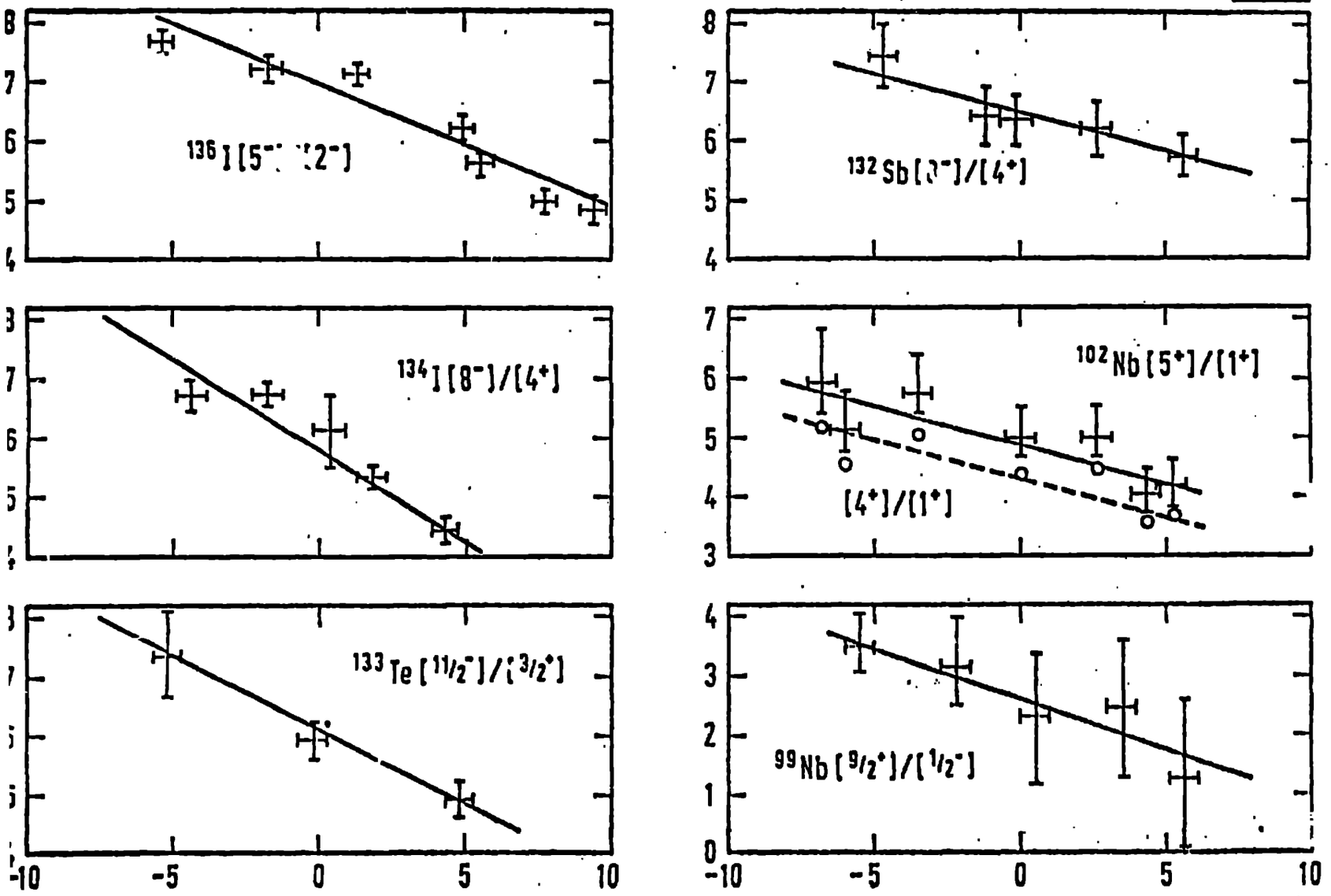
136 I [5⁻ : 2⁻]
132 Sb [3⁻]/[4⁺]
134 I [8⁻]/[4⁺]
102 Nb [5⁺]/[1⁺]
[4⁺]/[1⁺]
133 Te [11/2⁻]/[3/2⁺]
99 Nb [9/2⁺]/[1/2⁻]
-10
-5
0
5
10
E_k - Ē_k [MeV]

Fig. 9 $\bar{E}_k$

Table I: Decay Properties Used in the Evaluation of the Measurements [1].

Mass number	Nuclide	$T_{1/2}$[s]	E_ν[keV]	I_γ	P_1	P_2
99	Y	2.3(1.6)	122	0.409		
	Zr	2.0	468	0.576		
			546	0.460		
	Nb[1/2$^-$]	168	253	0.0791	0.2888	
			351	0.0592		
	Nb[9/2$^+$]	15	137	0.90(0.0214)	0.7112	
	Mo	66.0[h]				1
102 [2]	Zr	2.2	600	0.0751		
	Nb[high]	4.3	446	0.10	0.3269	
	Nb[low]	1.3	400	0.117	0.6731	
	Mo	690				1
132	Sn	40	247	0.417		
	Sb[8$^-$]	252	150	0.658	0	
	Sb[4$^+$]	168	974	1 (1)	1	
			696	0.69(1)		
	Te	77.8[h]	280	0.88		1
133	Sb	2.34[m]	1096	0.32		
	Te[11/2$^-$]	55.4 [m]	912	0.62	0.29	
	Te[3/2$^+$]	12.45[m]	312	0.70	0.71	0.16
	I	1248 [m]	530	0.89		0.84
134	Sb	11	297	0.97		
			1279	1		
	Te	2508	211	0.248		
			767	0.297		
	I[3$^+$]	228	272	0.79		
	I[4$^+$]	3156	847	0.9563	1	1
			884	0.654		
135	Te	18	603	0.254		
	I	6.59[h]	1260	0.286		
	Xe[11/2$^-$]	15.3 [m]	526	0.799	0.147	
	Xe[1/2$^+$]	9.17[h]	250	0.902	0.853	1

T a b l e I (continued):

Mass number	Nuclide	$T_{1/2}$[s]	E_γ[keV]	I_γ	P_1	P_2
136	Te	17.5	332	0.56		
	I[5$^-$]	46.0	381	1.0		
	I[2$^-$]	83.0	1313 1321	0.67(1) 0.2505	1	
	Xe	stable				1
137	Te	3.5	243	0.15		
	I	24.7	1219	0.134		
	Xe	229.8	455	0.31		

1)

$T_{1/2}$ Half-life of isotope.

E_γ Energy of γ-ray(s) evaluated.

I_γ Absolute line intersity of γ-ray (value in parentheses refers to the feeding on the same γ-ray in the decay of an isomer).

P_1 Fraction of β-decay to isomer indicated.

P_2 Fraction of decay of isomer to nuclide indicated.

2) Preliminary data, further radiochemical studies in progress.

Table II: Nanosecond Isomers Possibly Responsible for Higher-than-Average Ionic Charges of Fission Products in LOHENGRIN.

Fission Product of High Ionic Charge	Nanosecond-Isomer [20]
^{99}Zr	~15 ns - ^{99m}Zr
	~300 ns - ^{99m}Zr
^{99}Nb	7 ns isomer of mass 99 and unidentified Z
	100 ns isomer of mass 99 and unidentified Z
^{102}Nb	271 ns isomer of mass 102 and unidentified Z
	<4 ns - ^{102}Zr ?
^{133}Te	~85 ns isomer of mass 133 and unidentified Z
	750 ns isomer of mass 133 and unidentified Z
^{136}I	3 ns - ^{136m}I

Table III: Experimental Fractional Yields of Fission Products Indicated, and Corresponding Z_p- and EOF-Values Obtained by Fitting a Gaussian Curve Modulated by Odd-Even Factors.

A = 99 q = 21^+ $\bar{E}_k$ = 102.2[MeV] $\bar{\nu}$ = 1.54

E_k	Y	Zr	Nb[$1/2^-$]	Nb[$9/2^+$]	Z_p(σ=0.60)	EOF
96.7	13.8±2.0	58.9±7.3	15.8±3.9	11.5±4	40.15±0.08	1.00±0.17
100.0	22.7±2.5	59.2±8.0	11.5±3.5	6.6±4.4	39.95±0.09	0.98±0.17
102.7	31.3±3.7	55.5±6.0	10.7±3.0	2.5±2.0	39.81±0.10	0.95±0.16
105.7	39.5±4.0	49.4±6.1	8.7±4.0	2.4±2.0	39.72±0.11	0.88±0.17
107.8	49.1±3.9	39.8±5.0	10.9±4.5	0.5	39.66±0.12	0.75±0.17

A = 102 q = 22^+ $\bar{E}_k$ = 102.5[MeV] $\bar{\nu}$ = 1.40

E_k	Zr	Nb[high]	Nb[low]	Z_p(σ=0.56)	EOF=1.25
95.6	27.2±2.8	46.6±5.0	26.2±3.5	41.03±0.12	
96.5	26.5±2.8	40.7±4.3	32.8±3.5	41.05±0.14	
99.0	42.0±4.0	36.0±4.0	22.0±3.5	40.79±0.09	
102.5	51.1±5.5	26.2±4.6	22.7±3.5	40.63±0.10	
105.1	55.2±5.6	24.0±4.0	20.8±3.5	40.56±0.10	
106.8	55.1±5.6	17.9±4.0	27.0±3.5	40.56±0.12	
107.6	64.3±6.5	15.1±4.0	20.6±3.5	40.37±0.14	

A = 132 q = 23^+ $\bar{E}_k$ = 79.8 [MeV] $\bar{\nu}$ = 0.49

E_k	Sn	Sb[8^-]	Sb[4^+]	Te	Z_p(σ=0.56)	EOF
75.3	5.3±2.0	11.5±2.0	15.8±3.0	67,4±5	51.58±0.18	1.57±0.28
78.9	13.9±2.0	13.1±0.8	31.8±4.2	41.2±4	51.22±0.06	1.36±0.12
79.8	14.4±2.0	14.0±1.0	31.1±3.0	40.5±3.0	51.21±0.05	1.36±0.11
82.6	19.5±4.0	16.1±3.0	39.0±3.7	25.4±3.8	51.05±0.07	1.18±0.15
86.6	34.9±4.0	10.6±2.6	33.1±4.5	21.4±4.6	50.90±0.07	1.47±0.20

A = 133 q = 23^+ $\bar{E}_k$ = 78.5 [MeV] $\bar{\nu}$ = 0.65

E_k	Sb	Te[$11/2^-$]	Te[$3/2^+$]	Z_p(σ=0.56)	EOF=1.25
68.7	17.1±6.2	66.7±8.4	16.2±1.6	52.03±0.20	
73.3	28.9±3.2	49.8±4.2	21.3±1.2	51.75±0.12	
79.7	50.6±3.0	28.9±3.0	20.5±2.0	51.37±0.12	
83.4	66.9±1.5	15.4±2.0	17.7±1.0	51.17±0.16	

Table III (contd.)

A = 134 q = 23⁺ $\bar{E}_k$ = 77,2 [MeV] $\bar{\nu}$ = 0,85

E_k	Sb	Te	I	$Z_p(\sigma=0,47)$	EOF
71,7	4,3±0,2	71,8±0,2	23,9±0,2	52,26±0,02	1,18±0,02
75,4	4,4±0,2	80,9±1,4	14,7±1,4	52,18±0,03	1,41±0,03
79,0	7,3±1,2	83,8±2,0	9,0±0,8	52,03±0,04	1,44±0,11
81,3	7,0±0,4	87,3±3,4	5,8±2,2	51,97±0,07	1,65±0,30
84,7	10,4±0,6	82,5±3,6	7,1±3,2	51,94±0,09	1,39±0,25

A = 135 q = 24⁺ $\bar{E}_k$ = 75,0 [MeV] $\bar{\nu}$ = 0,93

E_k	Te	I	Xe	$Z_p(\sigma=0,56)$	EOF
70,2	29,2±1,3	66,8±1,3	4,0±2,0	52,61±0,09	0,75±0,10
71,5	43,1±1,4	53,4±1,4	3,5±2,0	52,50±0,10	0,90±0,12
73,0	44,3±1,7	52,4±1,7	3,3±2,0	52,49±0,08	0,91±0,13
75,0	60,2±2,3	37,3±2,3	2,5±2,0	52,35±0,05	1,00±0,04
75,7	64,1±2,4	33,4±2,4	2,5±2,0	52,28±0,05	0,99±0,04
78,5	78,4±2,7	19,8±2,7	1,8±2,0	52,07±0,07	1,05±0,04
78,8	75,5±1,8	23 ±1,8	1,5±2,0	52,13±0,06	1,04±0,04
81,2	84,0±4,0	15,5±4,0	0,5±2,0	51,95±0,07	1,04±0,10

A = 136 q = 24⁺ $\bar{E}_k$ = 74,0 [MeV] $\bar{\nu}$ = 1,07

E_k	Te	I[2⁻]	I[5⁻]	Xe	$Z_p(\sigma=0,56)$	EOF	
68,6	5,1±1,5	9,2±2,1	23,0±5,5	62,7±6,1	~~53,59±0,01~~	1,40±0,26	53,59 ± 0,18
72,5	11,9±3,0	13,6±2,9	28,8±5,9	45,9±11,5	53,27±0,10	1,38±0,18	
75,5	17,3±4,5	12,2±3,0	25,3±5,2	45,2±13,1	53,19±0,11	1,51±0,12	
79,5	19,6±4,9	17,6±3,0	20,2±4,3	42,6±4,3	53,15±0,12	1,63±0,15	

A = 137 q = 21⁺ $\bar{E}_k$ = 73,0 [MeV] $\bar{\nu}$ = 1,11

E_k	Te	I	Xe	$Z_p(\sigma=0,55)$	EOF	
65,8	3,0±0,2	32,6±3,0	58,4±7,3	~~53,32±0,04~~	1,60±0,25	53,38 ± 0,05
69,1	4,9±0,3	30,4±3,9	60,8±8,9	~~53,04±0,04~~	1,27±0,20	53,67 ± 0,06
69,3	5,3±0,2	29,7±3,6	58,3±8,1	~~53,14±0,04~~	1,28±0,21	53,41 ± 0,07
71,5	5,6±0,2	40,5±3,0	53,7±3,-	53,14±0,06	1,24±0,13	×
72,2	8,1±0,3	45,1±3,2	46,8±3,8	53,35±0,05	1,23±0,13	
72,7	7,0±0,3	40,4±3,7	52,6±3,5	53,40±0,05	1,29±0,19	
73,3	8,2±0,4	44,5±3,2	46,3±3,8	53,32±0,06	1,28±0,19	
75,5	10,9±0,5	45,5±3,5	43,6±3,9	53,28±0,05	1,29±0,19	
77,0	14,2±0,8	47,5±10,0	37,6±3,2	53,13±0,07	1,33±0,20	
77,2	13,6±1,0	44,5±10,3	37,2±3,2	53,14±0,06	1,43±0,23	
77,7	14,3±1,0	53,6±10,5	32,3±3,3	53,15±0,09	1,11±0,21	

Table III (Contd.)

A=134:	E_k	$F_h(^{134}I)$
	72,8	0,347±0,0029
	75,4	0,352±0,019
	77,5	0,283±0,066
	79,1	0,195±0,017
	81,5	0,096±0,007

A=135:	E_k	Xe[11/2⁻]	Xe[1/2⁺]
	72,0	2,34±0,15	< 3
	75,0	0,94±0,12	< 3
	75,7	0,67±0,08	< 3
	79,8	0,29±0,14	< 3

Explanation of symbols:

A mass number of chain

q ionic charge state of fragments separated

E_k mean kinetic energy of fragments from [43]

$\bar{\nu}$ number of prompt neutrons emitted from fragments of mass A from [20] [22]

E_k primary kinetic energy of fragment observed (corrected for energy loss in the target and by prompt neutron emission) [MeV]

F_h Fraction of independent yield of high spin isomer in relation to total independent yield of nuclide

Z_p, EOF, σ : see equations (1+2).

Table IV: Coefficients Describing the Change in Root Mean Square Angular Momentum (J_{rms}) with Fragment Kinetic Energy.

Fragment mass number (A)	$\Delta J_{rms}/\Delta E_k$ [$\hbar$/MeV]
99	$- 0.17 \pm 0.10$
102 $[5^+/1^+]$ +)	$- 0.13 \pm 0.05$
102 $[4^+/1^+]$ +)	$- 0.11 \pm 0.04$
132	$- 0.13 \pm 0.05$
133	$- 0.27 \pm 0.07$
134	$- 0.31 \pm 0.03$
136	$- 0.20 \pm 0.02$

+) obtained for the two assumed spin combinations; results of chain 102 are based on preliminary information on decay characteristics (see footnote to Table I).

References:

1. E.Moll,H.Schrader,G.Siegert,M.Asghar,J.P.Bocquet, G.Bailleul,J.P.Gautheron,J.Greif,G.I.Crawford,C.Chauvin, H.Ewald,H.Wollnik,P.Armbruster,G.Fiebig,H.Lawin,K.Sistemich, Nucl.Instr.and Methods 123,615(1975).
2. E.Moll,P.Armbruster,H.Ewald,G.Fiebig,H.Lawin,H.Wollnik, in Proc.Int.Conf.on electromagnetic isotope separators and the techniques of their applications, Marburg 1970. Report BMBW-FBK 70-28,241(1970).
3. E.Moll,G.Siegert,M.Asghar,G.Bailleul,J.P.Bocquet, J.P.Gautheron,J.Greif,H.Hammers,H.Schrader,P.Armbruster, G.Fiebig,H.Lawin,K.Sistemich,H.Ewald,H.Wollnik, in Proc. 8th Int.EMIS Conf.,Skövde,Sweden 1973,G.Anderson, G.Holmén Eds. (Gothenburg 1973) p.249.
4. G.Siegert,H.Wollnik,J.Greif,G.Fiedler,M.Asghar,G.Bailleul, J.P.Bocquet,J.P.Gautheron,H.Schrader,H.Ewald,P.Armbruster, Phys. Letters 53 B, 45 (1974).
5. G.Siegert,H.Wollnik,J.Greif,R.Decker,G.Fiedler,D.Pfeiffer, Phys.Rev. C 14, 1864 (1976).
6. H.Wollnik,G.Siegert,J.Greif,G.Fiedler, in Proceedings of the 3rd International Conference on Nuclei far from Stability,Cargèse(1976), Report CERN 76-13 (1976).
7. H.-G.Clerc,W.Lang,H.Wohlfarth,K.H.Schmidt,H.Schrader, in Proceedings of the 3rd International Conference on Nuclei far from Stability,Cargèse(1976), Report CERN 76-13(1976) and Report IKDA 76/5.
8. H.-G.Clerc,K.H.Schmidt,H.Wohlfarth,W.Lang,H.Schrader, K.E.Pferdekämper,R.Jungmann,M.Asghar,J.P.Bocquet, G.Siegert, Nuclear Physics A 247, 74 (1975).
9. H.-G.Clerc,W.Lang,H.Wohlfarth,K.H.Schmidt,H.Schrader, K.E.Pferdekämper,R.Jungmann, Z.Physik A 274,203(1975).
10. H.Wohlfarth,W.Lang,H.-G.Clerc,H.Schrader,K.H.Schmidt, H.Dann, Physics Letters 63 B, 275 (1976).
11. H.-G.Clerc,W.Lang,H.Wohlfarth,H.Schrader,K.H.Schmidt, these proceedings, contribution F 2.
12. H.O.Denschlag et al., to be published.
13. H.W.Schmitt,J.H.Neiler,F.J.Walter,Phys.Rev.141,1146(1966).
14. K.Debertin,U.Schötzig, submitted to Nucl. Instr. and Methods (1978).
15. R.J.Gehrke,R.G.Helmer,R.C.Greenwood,Nucl. Instr. and Methods 147, 405 (1977).
16. Nuclear Data Sheets.
17. Table of Isotopes,C.M.Lederer,V.S.Shirley(Eds.),Wiley, (New York)(1978).
18. G.Siegert,J.Greif,H.Wollnik,R.Decker,G.Fiedler,W.Kaiser, D.Pfeiffer, Report AED-Conf-76-072-007.

19. H.Wohlfarth,W.Lang,H.Dann,H.-G.Clerc,K.H.Schmidt, H.Schrader, Report IKDA 78/6.

20. R.G.Clark,L.E.Glendenin,W.C.Talbert Jr., in Physics and Chemistry of Fission (Proc. Symposium Rochester, 1973), Vol.II,p.221.

21. B.F.Rider,M.E.Meek, Compilation of Fission Product Yields, Report NEDO-12154-2(D)(1977).

22. A.C.Wahl,A.E.Norris,R.A.Rouse,J.C.Williams, in Physics and Chemistry of Fission (Proc. Symposium Vienna, 1969), IAEA,Vienna (1969),p.813.

23. S.Amiel,H.Feldstein, in Physics and Chemistry of Fission (Proc. Symposium Rochester, 1973), IAEA,Vienna (1974), Vol.II,p.65.

24. A.C.Wahl, Contribution to Second Advisory Group Meeting on Fission Product Nuclear Data, IAEA Petten, to appear as Report INDC-(NDS)-87,p.215-244. [(1977)

25. R.Vandenbosch,J.R.Huizenga, Nuclear Fission, Academic Press, New York (1973).

26. B.D.Wilkins,E.P.Steinberg,R.R.Chasman,Phys.Rev. C 14,1832, (1976).

27. H.Nifenecker,G.Signarbieux,R.Babinet,J.Poitou,in Physics and Chemistry of Fission (Proc. Symposium Rochester,1973) IAEA,Vienna (1974) Vol.II,p.117.

28. J.R.Huizenga,R.Vandenbosch, Phys.Rev.120,1305(1960).

29. R.Vandenbosch,J.R.Huizenga, Phys.Rev.120,1313(1960).

30. D.G.Madland,T.R.England, Nucl.Sci.Eng.64,859(1977), and Report LA-6595-Ms(1976).

31. J.B.Wilhelmy,E.Cheifetz,R.C.Jared,S.G.Thompson,H.R.Bowman, J.O.Rasmussen, Phys.Rev. C 5, 2041 (1972).

32. M.Weis, Doctoral thesis, Mainz 1979.

33. J.R.Nix,W.J.Swiatecki, Nucl.Phys.71,1(1965).

34. J.O.Rasmussen,W.Nörenberg,H.J.Mang, Nucl.Physics A 136, 456 (1969).

H. O. Denschlag, H. Braun, W. Faubel, G. Fischbach, H. Meixler,
G. Paffrath, W. Pörsch, M. Weis (Institut für Kernchemie,
Universität Mainz, D-6500 Mainz, Germany),
H. Schrader, G. Siegert (Institut Laue-Langevin, Grenoble),
J. Blachot (Centre d'Etudes Nucléaires, Grenoble, France),
Z. B. Alfassi[+] (Ben Gurion University, Beer Sheva, Israel),
H. N. Erten[+] (Middle East Technical Univ., Ankara, Turkey),
T. Izak-Biran[+] (Soreq Nucl. Research Centre, Yavne, Israel),
T. Tamai[+] (Kyoto Univ. Research Reactor Institute, Japan),
A. C. Wahl[+] (Washington University, St. Louis, Missouri, USA),
K. Wolfsberg[+] (Los Alamos Sci. Lab., Los Alamos, N.M. USA)., CNC-11

[+] Guest scientist at Universität Mainz.